Eur. Phys. J. C 35, 171–176 (2004)
Digital Object Identifier (DOI) 10.1140/epjc/s2004-01867-4

THE EUROPEAN PHYSICAL JOURNAL C

Determining resonance parameters of heavy Higgs bosons at a future linear collider

N. Meyer[1,2], K. Desch[1]

[1] Institut für Experimentalphysik, Universität Hamburg, Luruper Chaussee 149, 22761 Hamburg, Germany
[2] DESY, Notkestraße 85, 22607 Hamburg, Germany

Received: 13 February 2004 / Revised version: 14 April 2004 /
Published online: 18 May 2004 –

Abstract. This study investigates the potential of an Electron-Positron Linear Collider for measuring resonance parameters of Higgs bosons beyond the mass range studied so far. The analysis is based on the reconstruction of events from the Higgs-strahlung process $e^+e^- \to HZ$. It is shown that the total width Γ^H_{tot}, the mass m_H and the event rate N can be measured from the mass spectrum in a model independent way. Also, the branching ratios BR^H_{WW} and BR^H_{ZZ} can be measured, assuming these are the only relevant Higgs decay modes. The simulation includes realistic detector effects and all relevant Standard Model background processes. Results are given for $m_H = 200$–$320\,GeV$ assuming $\int\mathcal{L} = 500\,fb^{-1}$ integrated luminosity at a collision energy $\sqrt{s} = 500\,GeV$.

1 Introduction

During the past years many simulations have been performed to investigate the prospects of measuring Higgs boson properties [1] at future Linear Colliders [2–4]. The main focus was put on Higgs masses m_H below the WW-threshold which is the mass region preferred by recent electroweak data [5].

In high energy e^+e^- collisions Higgs bosons can be produced in two dominant production processes: Higgs-strahlung $e^+e^- \to HZ$ [6] and WW-fusion $e^+e^- \to H\nu_e\bar{\nu}_e$ [7], see Fig. 1. As can be seen from Fig. 2, Higgs-strahlung with $\sigma_{HZ} \sim 1/s$ dominates for lower collision energies, while WW-fusion becomes the major production mode, due to its $\sigma_{H\nu_e\bar{\nu}_e} \sim \log s$ cross-section rise [9], if $\sqrt{s}$ is large compared to m_H.

Higgs bosons couple proportionally to mass and therefore are generally predicted to decay into the heaviest particles possible. In the Standard Model (SM) and most of its extensions, the total Higgs decay width is expected to be very small for Higgs masses below the WW-threshold. Figure 3 shows the SM prediction. Only if the Higgs width is as large as few GeV, it can be determined from the observed Higgs line-shape. This is not possible for smaller widths due to limited detector resolution. However, it is possible to determine the width in a model independent way using the relations $\Gamma^H_{tot} = \Gamma^H_{\gamma\gamma}/BR^H_{\gamma\gamma}$ [11] or $\Gamma^H_{tot} = \Gamma^H_{WW}/BR^H_{WW}$ [12].

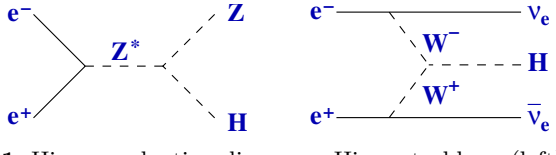

Fig. 1. Higgs production diagrams: Higgs-strahlung (left) and WW-fusion (right)

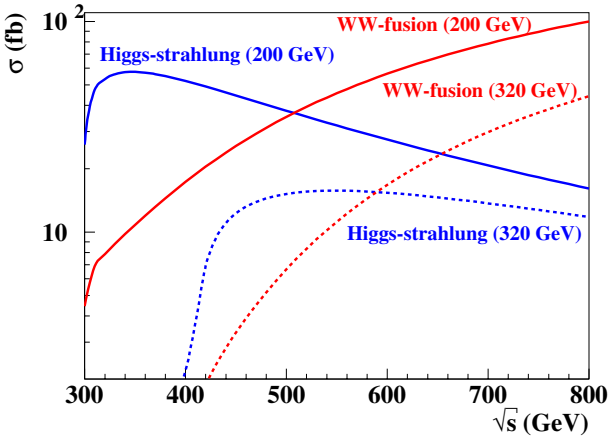

Fig. 2. Standard Model production cross sections for Higgs-strahlung und WW-fusion, calculated with `HZHA` [8]. Numbers in brackets indicate different choices for the Higgs mass. Interference between common $H\nu_e\bar{\nu}_e$ final states is negligible

From the line-shape it is possible to determine the width, the mass and the event rate in a model-independent way. The signal and background processes studied are specified in Sect. 2. Event selection is described in Sect. 3 followed by the methods of estimating detector resolution in Sect. 4. For this, a separation of $H \to WW$ and $H \to ZZ$ decays is necessary, which can be interpreted as branching fraction measurements assuming that there are no other major decay modes. The note continues with details on the reconstruction of Higgs resonance parameters in Sect. 5. Results are summarized and discussed in Sect. 6.

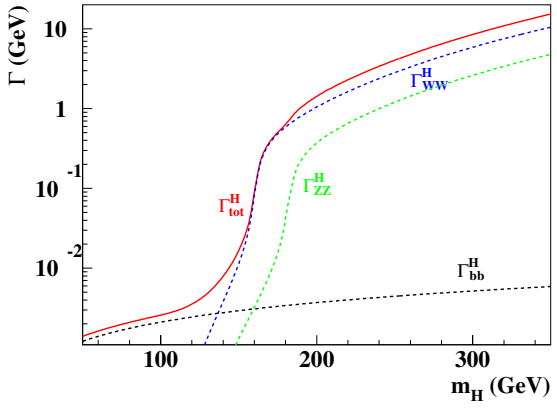

Fig. 3. Standard Model prediction for the total Higgs width $\Gamma^{\mathrm{H}}_{tot}$, calculated with `HDECAY` [10]. Also shown are the partial widths $\Gamma^{\mathrm{H}}_{\mathrm{bb}}$, $\Gamma^{\mathrm{H}}_{\mathrm{WW}}$ and $\Gamma^{\mathrm{H}}_{\mathrm{ZZ}}$ of the dominant decay modes

2 Signal and background

Higgs bosons with Standard Model couplings are studied in the mass range from $m_{\mathrm{H}} = 200\,\mathrm{GeV}$ to 320 GeV, where both cross section and width are large enough for precision measurements.

In this mass range, SM Higgs bosons decay almost exclusively into pairs of massive gauge bosons. The successive decays are classified in terms of final state signatures in Table 1.

For final states with neutrinos, constraint fits often used to enhance mass resolution are difficult. Thus, channels 1, 2, 4 and 6 from Table 1 are not used for high precision mass reconstruction. Among the fully detectable final states, channel 3 is by far the most dominant. However, this is also the channel where the largest background contaminations are expected (e.g. $\mathrm{e^+e^-} \to \mathrm{t\bar{t}}$). On the contrary, the gold-plated channel with six leptons in the final state is too rare for precision measurements. Channel 5 with one leptonic Z-decay and hadronic W- or Z-pair decays is a good compromise between signal rate and background contamination.

Table 1. Signal final states and their occurrence. Numbers given are estimates using typical values for cross section $\sigma_{\mathrm{HZ}} = 45\,\mathrm{fb}$ and branching ratios $\mathrm{BR}^{\mathrm{H}}_{\mathrm{WW}} = 0.7$, $\mathrm{BR}^{\mathrm{H}}_{\mathrm{ZZ}} = 0.3$. Here, ℓ is any charged lepton flavor and q any quark flavor kinematically allowed

	$\mathrm{e^+e^-}$ $\to$	Final state	H $\to$ WW	H $\to$ ZZ	Ratio	Events per $500\,\mathrm{fb}^{-1}$
1.	$\mathrm{H}\nu_{\mathrm{e}}\bar{\nu}_{\mathrm{e}}$	$2\nu + X$	×	×	100 %	15000
2.	HZ	$2\nu + X$	×	×	35.1 %	7895
3.	HZ	qq qq qq	×	×	34.3 %	7720
4.	HZ	qq qq $\ell\nu$	×		19.2 %	4315
5.	HZ	$\ell\ell$ qq qq	×	×	7.84 %	1765
6.	HZ	$\ell\ell$ qq $\ell\nu$	×		2.94 %	660
7.	HZ	$\ell\ell\,\ell\ell$ qq		×	0.63 %	140
8.	HZ	$\ell\ell\,\ell\ell\,\ell\ell$		×	0.03 %	5

Events containing τ leptons do not pass the selection criteria described in Sect. 3 without dedicated τ identification. Therefore, only events with $\ell = \mathrm{e}, \mu$ are taken into account. All background processes with two charged leptons plus jets are considered. They can be classified as follows:

6f Six fermion processes, $\mathrm{e^+e^-} \to 2\ell$ 4q, yield events with the same final state as signal events. As will be shown later, this is the dominant class of background processes.

4f Four fermion processes including ZZ-pair production, $\mathrm{e^+e^-} \to 2\ell$ 2q. This class of processes seems problematic because of huge cross sections. However, event topology differs from signal events.

$\mathrm{t\bar{t}}$ Top quark pair production, $\mathrm{e^+e^-} \to \mathrm{t\bar{t}} \to \mathrm{b\bar{b}W^+W^-}$. Here, high energetic leptons can occur in W- as well as in b-decays. Therefore, all decays $\mathrm{W} \to \mathrm{q\bar{q}}$ and $\mathrm{W} \to \ell\nu$ are considered. Again it is not event topology but large cross section which makes this background a cause for concern.

Other processes (e.g. $\mathrm{e^+e^-} \to \mathrm{WW} \to \mathrm{qq}\ell\nu$) are expected to be negligible due to missing isolated leptons, large missing energy or low mass of the hadronic system.

Signal as well as background events are generated using `WHiZard 1.22` [13], except $\mathrm{t\bar{t}}$-events for which `PYTHIA 6.2` [14] is used. Both initial state radiation and beamstrahlung [15] are taken into account. For this analysis, no significant signal over background enhancement is expected for polarized beams, so the possibility of beam polarization is not studied. Except for $\mathrm{e^+e^-} \to \mathrm{t\bar{t}}$, cuts on fermion-pair invariant masses $m_{\ell\ell,\,\mathrm{qq}} > 10\,\mathrm{GeV}$ for any lepton-/quark-pair are applied during the generation of Monte Carlo (MC) events.

Detector response is estimated using the fast simulation `SIMDET 4` [16] which parameterizes detector performance as described in the TESLA TDR [2].

3 Event selection

In all events a search is made for energy flow objects which are classified as lepton (electron or muon). The most energetic of these objects is combined with any other identified lepton. The pair with invariant mass closest to m_{Z} is selected as $\mathrm{Z} \to \ell\ell$ candidate and removed from the event. All other energy flow objects are forced to four jets by the Durham recombination scheme [17].

The invariant mass of the two leptons must be close to the Z mass, $|m_{\ell\ell} - m_{\mathrm{Z}}| < 5\,\mathrm{GeV}$ and the hadronic part of the event should consist of four jets, $y_{34} > 10^{-3}$. All leptons and jets must be well inside the detector, $|\cos\theta_\ell| < 0.99$ for leptons and $|\cos\theta_{\mathrm{jet}}| < 0.95$ for jets. Since $m_{\mathrm{H}} > m_{\mathrm{Z}}$, the energy of the lepton pair is required to be $E_{\ell\ell} < 225\,\mathrm{GeV} = 0.45\sqrt{s}$, to reduce events from Z-pair production.

As a last selection step, a kinematic fit is applied. This fit imposes energy and momentum conservation, allows for longitudinal momentum imbalance due to initial photon radiation and requires two jet pairs to have same invariant masses. The latter constraint also defines the assignment of

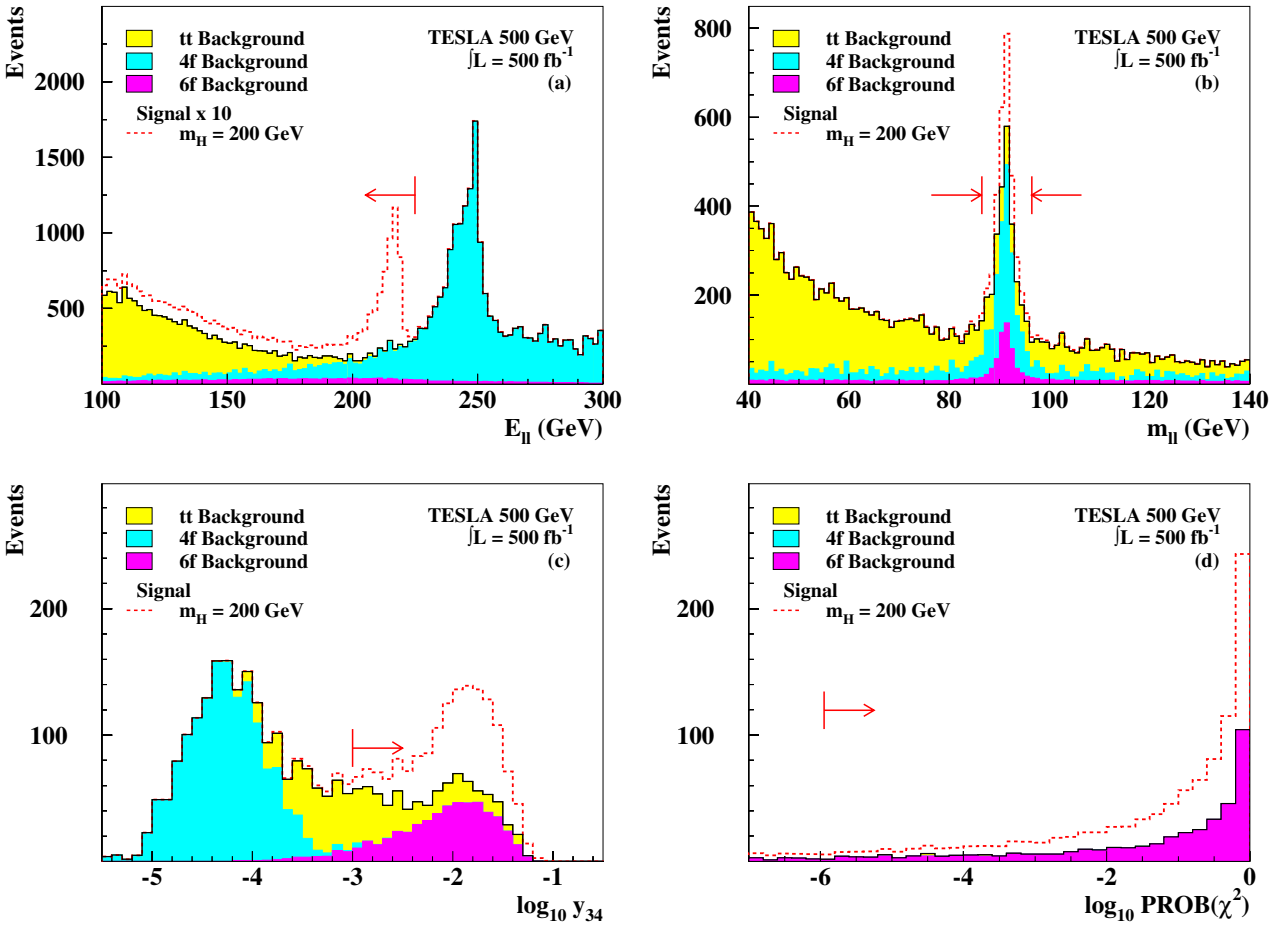

Fig. 4. Distributions of di-lepton energy $E_{\ell\ell}$ (**a**), di-lepton mass $m_{\ell\ell}$ (**b**), jet separation parameter y_{34} (**c**) and χ^2-probability of the kinematic fit $PROB(\chi^2)$ (**d**) before the corresponding cuts. The expected HZ signal, added to the background, is shown as dashed line. Note that the signal is scaled by factor 10 in (**a**)

Table 2. Evolution of event rates through the selection. Main remaining background source are events from 6f processes $e^+e^- \to 2\ell\,4q$. Event rates in the first line include MC level cuts as described in the text

		Signal m_H [GeV]				Background		
	Variable (range)	200	240	280	320	6f	4f	$t\bar{t}$
	Events / 500 fb^{-1}	1120	880	630	410	4340	392 000	240 000
1.-3.	$\geq 2\ell$, $\cos\theta_\ell$, $\cos\theta_{\rm jet}$	904	706	498	322	1803	38 000	90 000
4.	$E_{\ell\ell}$ (< 225 GeV)	897	705	497	321	1512	5764	90 000
5.	$m_{\ell\ell}$ ($m_Z \pm 10$ GeV)	770	600	425	275	369	1506	750
6.	y_{34} ($> 10^{-3}$)	745	581	413	268	343	5	357
7.	PROB(χ^2) ($> 10^{-6}$)	585	463	333	216	271	0	4
	Efficiency	52 %	53 %	53 %	53 %			

the jets to two intermediate particles assumed to be either a pair of W- or Z-bosons. Thus, together with the lepton-pair, each event consists of three reconstructed gauge bosons.

Table 2 shows the overall performance of the event selection. In addition, the distributions of the most important variables used for background suppression are displayed in Fig. 4. Background suppression is possible to $S/B \sim 1$ or better depending on the Higgs mass. Events from four fermion processes and $t\bar{t}$-pair production can be rejected almost completely. Signal efficiency ϵ_{signal} is stable as a function of m_H and is always larger than 50 %.

4 Separation of H → WW and H → ZZ

Since it is a priori unknown which two of the three bosons originate from the Higgs decay, a distribution is formed which contains all three possible di-boson masses per event.

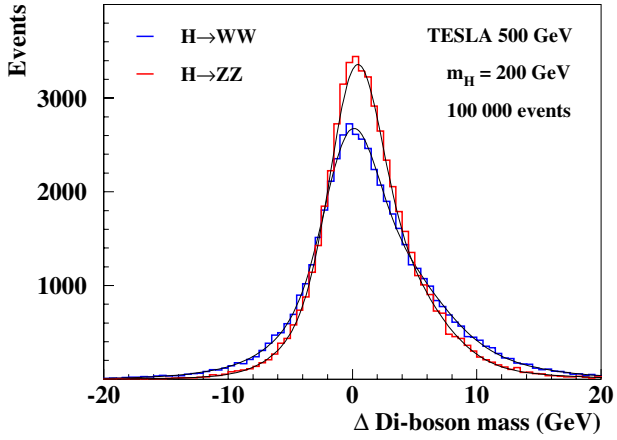

Fig. 5. Di-boson mass resolution from MC with $\Gamma^{\mathrm{H}}_{tot} = 0\,\mathrm{GeV}$. As can be seen, resolutions differ for $\mathrm{H} \to \mathrm{WW}$ and $\mathrm{H} \to \mathrm{ZZ}$. Both distributions are asymmetric due to the constraints of the kinematic fit. The difference in normalization results in the different selection efficiencies

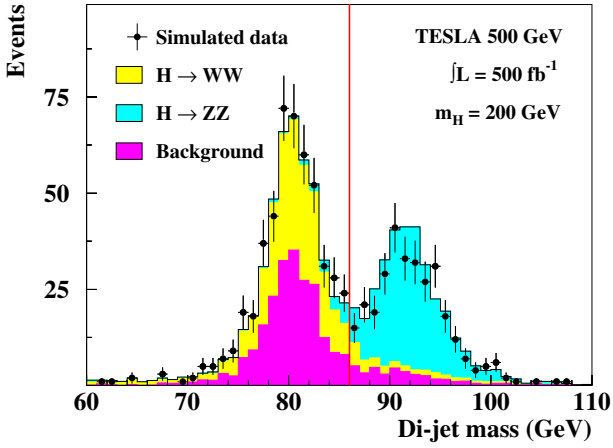

Fig. 6. Di-jet mass spectrum as obtained from the kinematic fit. Clearly visible are two peaks at m_{W} and m_{Z} respectively

It is expected that the correct pairing will exhibit a mass peak while the two wrong combinations will form a flat combinatoric background.

In order to determine the resonance parameters (μ, Γ, N) from this distribution, the Breit-Wigner shape of the resonance has to be convoluted with a properly tuned detector resolution function. The detector resolution differs for events from $\mathrm{H} \to \mathrm{ZZ}$ (where the correct di-boson mass partially is an invariant mass from $\ell\ell\,\mathrm{qq}$) and from $\mathrm{H} \to \mathrm{WW}$ (where it is always from $\mathrm{qq}\,\mathrm{qq}$). The expected mass spectra and the parameterizations[1] used for convolution are shown in Fig. 5 for $m_{\mathrm{H}} = 200\,\mathrm{GeV}$. Resolutions for the other Higgs masses are similar.

Events from the two Higgs decays enter the di-boson mass spectrum with relative fractions

$$RF_{\mathrm{WW}} = \frac{N_{\mathrm{WW}}}{N_{\mathrm{WW}} + N_{\mathrm{ZZ}}} \quad \text{and} \quad RF_{\mathrm{ZZ}} = \frac{N_{\mathrm{ZZ}}}{N_{\mathrm{WW}} + N_{\mathrm{ZZ}}},$$

respectively, with N_i being the number of events for each channel after selection. The fractions RF_{WW} and RF_{ZZ} are determined from the di-jet mass as obtained from the kinematic fit. An example distribution for $m_{\mathrm{H}} = 200\,\mathrm{GeV}$ is shown in Fig. 6, where two peaks from W- and Z-decays respectively are clearly visible.

The di-jet mass spectrum is divided by a mass cut, chosen to be $m^{cut}_{jj} = 85.8\,\mathrm{GeV}$. Events above this mass cut mainly originate from $\mathrm{H} \to \mathrm{ZZ}$ decays. Below the cut, the sample consists of $\mathrm{H} \to \mathrm{WW}$ decays with a significant background contribution. From the number of events above and below m^{cut}_{jj}, the relative fractions of $\mathrm{H} \to \mathrm{WW}$ and $\mathrm{H} \to \mathrm{ZZ}$ decays can be extracted in a model independent way. In addition, assuming there are only Higgs decays to W- or Z-pairs, the corresponding branching ratios $\mathrm{BR}^{\mathrm{H}}_{\mathrm{WW}}$ and $\mathrm{BR}^{\mathrm{H}}_{\mathrm{ZZ}}$ can be calculated. Table 3 resumes statistical errors on relative fractions and branching ratios as expected from $\int\mathcal{L} = 500\,\mathrm{fb}^{-1}$ of data.

Table 3. Results for relative fractions and branching ratios. Numbers given are mean values of 100 independent Monte Carlo experiments corresponding to an integrated luminosity of $\int\mathcal{L} = 500\,\mathrm{fb}^{-1}$ each

m_{H} [GeV]	$\frac{\Delta RF_{\mathrm{WW}}}{RF_{\mathrm{WW}}}$	$\frac{\Delta RF_{\mathrm{ZZ}}}{RF_{\mathrm{ZZ}}}$	$\frac{\Delta \mathrm{BR}^{\mathrm{H}}_{\mathrm{WW}}}{\mathrm{BR}^{\mathrm{H}}_{\mathrm{WW}}}$	$\frac{\Delta \mathrm{BR}^{\mathrm{H}}_{\mathrm{ZZ}}}{\mathrm{BR}^{\mathrm{H}}_{\mathrm{ZZ}}}$
200	7.3 %	5.7 %	3.5 %	9.9 %
240	8.9 %	7.0 %	5.0 %	10.8 %
280	11.9 %	9.3 %	7.7 %	16.2 %
320	15.2 %	12.0 %	8.6 %	17.3 %

5 Reconstruction of Higgs resonance parameters

Finally, the spectrum of the reconstructed di-boson masses is built. Each event yields three entries for the different combinations possible. This spectrum can be reduced to the following parts:

1. The correct combination of di-bosons form a clear peak. This peak can be described as a Breit-Wigner function convoluted with the detector resolution. The Breit-Wigner parameters μ, Γ and N are free parameters of the fit, while the parameters of the detector resolution are fixed from MC.
2. The wrong combinations of di-boson masses form a flat combinatoric background. The shape is parameterized by a step function whose parameters are fixed from the same MC sample as the detector resolution[2] while the number of entries is determined in the fit by the free parameter N of the Higgs peak Breit-Wigner function.

[1] Detector effects are parameterized separately for $\mathrm{H} \to \mathrm{WW}$ and $\mathrm{H} \to \mathrm{ZZ}$ by multi-Gaussian functions. The choice is arbitrary and motivated by the good agreement between MC and parameterization.

[2] Here it is assumed that the shape of the combinatoric background does not depend on the Higgs width.

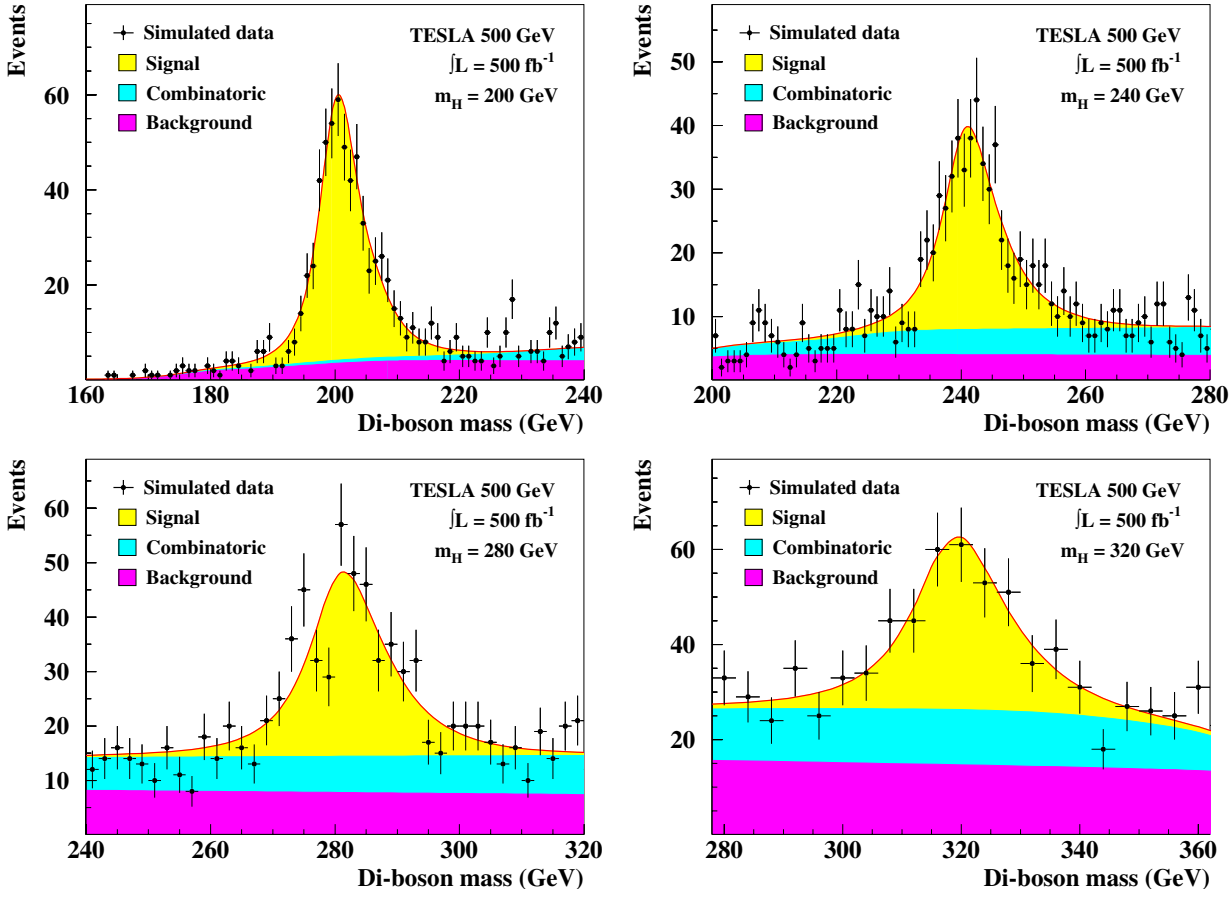

Fig. 7. Di-boson mass spectra for the four Higgs masses under study. Everywhere, the Higgs resonances are clearly visible over physical and combinatoric background for $\int\mathcal{L} = 500\,\mathrm{fb}^{-1}$ of integrated luminosity at $\sqrt{s} = 500\,\mathrm{GeV}$

3. In addition, there is a flat distribution from background events which remain after the selection criteria. This physical background is parameterized in the same way as the combinatoric background. Besides the parameters for the shape, in this case also the number of entries is fixed by MC expectation[3].

Figure 7 shows the distributions of reconstructed di-boson masses with the fitted function. The fit parameters $\mu = m_\mathrm{H}, \Gamma = \Gamma^\mathrm{H}_{tot}$ and $N = \sigma \times \mathrm{BR} \times \epsilon$ are determined from 100 independent MC experiments, each corresponding to $500\,\mathrm{fb}^{-1}$ of integrated luminosity. Both the mean value and the spread of all results lie within statistical expectations. The average expected relative measurement errors are listed in Table 4.

Table 4. Expected relative errors on event rate N, Higgs mass m_H and Higgs width Γ^H_{tot} as fitted to the di-boson mass spectrum. Also listed are results for the branching ratios $\mathrm{BR}^\mathrm{H}_{\mathrm{WW}}$ and $\mathrm{BR}^\mathrm{H}_{\mathrm{ZZ}}$ as described in Sect. 4. All numbers are mean values obtained with 100 independent signal samples corresponding to $\int\mathcal{L} = 500\,\mathrm{fb}^{-1}$ at $\sqrt{s} = 500\,\mathrm{GeV}$ each

m_H [GeV]	$\frac{\Delta N}{N}$	$\frac{\Delta m}{m}$	$\frac{\Delta\Gamma}{\Gamma}$	$\frac{\Delta \mathrm{BR}^\mathrm{H}_{\mathrm{WW}}}{\mathrm{BR}^\mathrm{H}_{\mathrm{WW}}}$	$\frac{\Delta \mathrm{BR}^\mathrm{H}_{\mathrm{ZZ}}}{\mathrm{BR}^\mathrm{H}_{\mathrm{ZZ}}}$
200	3.6 %	0.11 %	34.0 %	3.5 %	9.9 %
240	3.8 %	0.17 %	26.8 %	5.0 %	10.8 %
280	4.4 %	0.24 %	22.7 %	7.7 %	16.2 %
320	6.3 %	0.36 %	26.4 %	8.6 %	17.3 %

6 Summary and conclusion

A method to reconstruct the resonance parameters of a Higgs boson produced in Higgs-strahlung at a future Linear Collider is presented. From the observed line-shape, the decay width Γ^H_{tot}, the mass m_H and the event rate N are derived from a model-independent fit. The method is restricted to Higgs bosons with Γ^H_{tot} in excess of a few GeV. In the Standard Model, this is the case for $m_\mathrm{H} \gtrsim 200\,\mathrm{GeV}$. Assuming the Higgs only decays to W- and Z-boson pairs, determination of the corresponding branching ratios $\mathrm{BR}^\mathrm{H}_{\mathrm{WW}}$ and $\mathrm{BR}^\mathrm{H}_{\mathrm{ZZ}}$ is possible as well. The results from 100 independent MC experiments each corresponding to $\int\mathcal{L} = 500\,\mathrm{fb}^{-1}$ lie within statistical expectation.

This analysis has been optimized for the reconstruction of the decay width. The expected relative measurement error on Γ^H_{tot} is within 23–34 %, varying with the

[3] In later experiments, the background parameters can be determined off-peak in data.

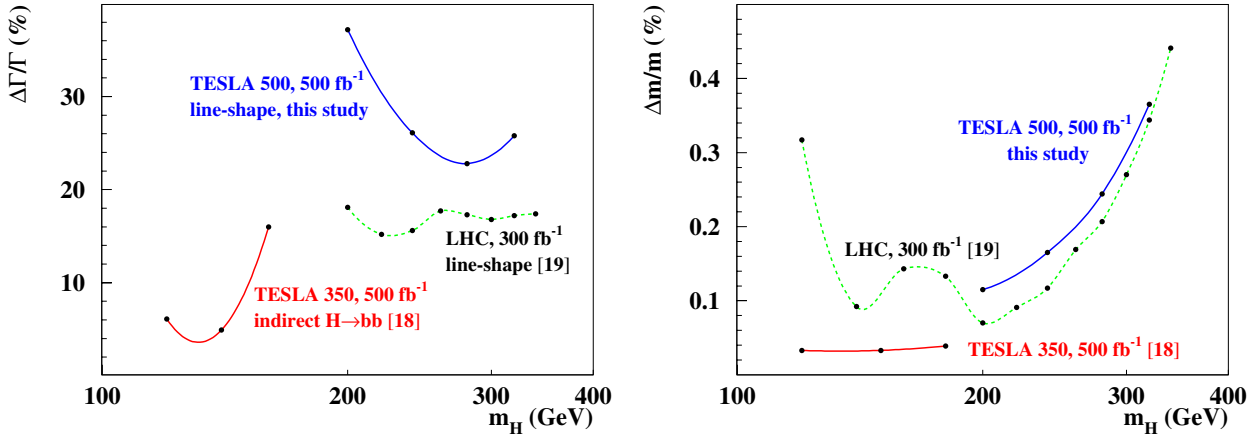

Fig. 8. Expected errors of measurement simulations on Higgs width (left) and mass (right) at Linear Collider and LHC. Only statistical uncertainties are shown

Higgs mass. In Fig. 8 (left), the result is shown together with the result from an indirect method applied to $m_H = 120$–$160\,\text{GeV}$ [12][4] and from line-shape reconstruction at LHC [19]. Statistical precision is slightly better at LHC for $300\,\text{fb}^{-1}$ of integrated luminosity. However, systematic shifts of the reconstructed Higgs width, which are of the same order as the statistical uncertainty, are not taken into account in [19].

The expected errors on Higgs mass, event rate and branching ratios presented here are the first results from Linear Collider studies available for Higgs masses larger than 160 GeV. They are very promising for dedicated analyses on these observables still to be studied. As an example, in Fig. 8 (right) the expected error on m_H from this study is shown together with the result from a dedicated Linear Collider study for lower masses [18] and from LHC line-shape reconstruction [19].

Acknowledgements. This work has been supported in part by the DFG Graduate School No. 602 "Future Developments in Particle Physics" at the University of Hamburg.

References

1. P.W. Higgs, Phys. Lett. **12**, 132 (1964); P.W. Higgs, Phys. Rev. Lett. **13**, 508 (1964); P.W. Higgs, Phys. Rev. **145**, 1156 (1966); F. Englert, R. Brout, Phys. Rev. Lett. **13**, 321 (1964); G.S. Guralnik, C.R. Hagen, T.W.B. Kibble, Phys. Rev. Lett. **13**, 585 (1964)
2. J.A. Aguilar-Saavedra et al., TESLA Technical Design Report Part III: Physics at an e^+e^- Linear Collider, arXiv:hep-ph/0106315.
3. T. Abe et al., Proc. of the APS/DPF/DPB Summer Study on the Future of Particle Physics (Snowmass 2001), ed. N. Graf, SLAC-R-570
4. K. Abe et al., Particle physics experiments at JLC, arXiv:hep-ph/0109166
5. [LEP Collaboration], A combination of preliminary electroweak measurements and constraints on the standard model, arXiv:hep-ex/0312023
6. J.R. Ellis, M.K. Gaillard, D.V. Nanopoulos, Nucl. Phys. B **106**, 292 (1976); J.D. Bjorken, Proc. 1976 SLAC Summer Inst. Part. Phys., ed. M.C. Zipf (SLAC report 198, 1977) 1; B.W. Lee, C. Quigg, H.B. Thacker, Phys. Rev. D **16**, 1519 (1977); B.L. Ioffe, V.A. Khoze, Sov. J. Part. Nucl. **9**, 50 (1978); D.R.T. Jones, S.T. Petcov, Phys. Lett. B **84**, 440 (1979); F.A. Berends, R. Kleiss, Nucl. Phys. B **260**, 32 (1985)
7. R.N. Cahn, S. Dawson, Phys. Lett. B **136**, 196 (1984); G.L. Kane, W.W. Repko, W.B. Rolnick, Phys. Lett. B **148**, 367 (1984); G. Altarelli, B. Mele, F. Pitolli, Nucl. Phys. B **287**, 205 (1987); W. Kilian, M. Kramer, P.M. Zerwas, Phys. Lett. B **373**, 135 (1996)
8. P. Janot, in Physics at LEP, eds. G. Altarelli, T. Sjöstrand, F. Zwirner, CERN 96-01, Vol. 2 (1996) 309
9. A. Djouadi, J. Kalinowski, P. Ohmann, P.M. Zerwas, Z. Phys. C **74**, 93 (1997)
10. A. Djouadi, J. Kalinowski, M. Spira, Comput. Phys. Commun. **108**, 56 (1998)
11. G. Jikia, S. Söldner-Rembold, Proceedings of the 7th International Workshop on High Energy Photon Colliders, Hamburg 2000, 133; M. Melles, W.J. Stirling, V.A. Khoze, Phys. Rev. D **61**, 054015 (2000)
12. K. Desch, N. Meyer, Study of Higgs Boson Production through WW-fusion at TESLA, LC-PHSM-2001-025
13. W. Kilian, WHiZard 1.22 - Manual, LC-TOOL-2001-039
14. T. Sjostrand et al., Comput. Phys. Commun. **135**, 269 (2001)
15. T. Ohl, Comput. Phys. Commun. **101**, 269 (1997)
16. M. Pohl, H.J. Schreiber, SIMDET - Version 4: A parametric Monte Carlo for a TESLA detector, DESY 02-061, arXiv:hep-ex/0206009
17. Y. Dokshitzer, J. Phys. G **17**, (1991), 1537; N. Brown, W.J. Stirling, Phys. Lett. B **252**, 657 (1990); S. Bethke et al., Nucl. Phys. B **370**, 310 (1992); S. Catani et al., Phys. Lett. **B269** (1991),432; N. Brown, W.J. Stirling, Z. Phys. C **53**, 629 (1992)
18. P. Garcia-Abia, W. Lohmann, A. Raspereza, Measurement of the Higgs Boson Mass and Cross Section with a Linear e^+e^- Collider, LC-PHSM-2001-054
19. V. Drollinger, A. Sopczak, Eur. Phys. J. direct C **3** (2001) N1

[4] The method is also applicable for $m_H > 160\,\text{GeV}$ exploiting $H \to WW$, however this has not yet been studied in detail.